
Generalized Conductor-like Screening Model (GCOSMO) for Solvation: An Assessment of Its Accuracy and Applicability

THANH N. TRUONG,* UYEN N. NGUYEN, AND EUGENE V. STEFANOVICH†

Department of Chemistry, University of Utah, Salt Lake City, Utah 84112

Received March 28, 1996; revised manuscript received May 27, 1996; accepted May 29, 1996

ABSTRACT

We present an assessment on the accuracy of a dielectric continuum solvation model, the generalized conductor-like screening model (GCOSMO), for predicting hydration free energies, tautomeric equilibria, and reaction profiles in solution. © 1996 John Wiley & Sons, Inc.

Introduction

For the past half century, quantum chemistry has made significant progress in the development of theory as well as its applications to predict physical properties of gas-phase processes. Recently, theoretical efforts have been shifting focus toward solution chemistry. In particular, many theoretical approaches have been proposed for modeling solvation. The dielectric continuum ap-

proach [1–3], however, offers the simplest methodology for incorporating solvent effects into a wide range of ab initio molecular orbital (MO) and density functional theory (DFT) levels of theory. In the dielectric continuum approach, the solvated system is modeled as the solute inside a cavity surrounded by a dielectric continuum medium characterized by the dielectric constant ϵ . Models based on molecular-shape cavities have been shown to provide a more accurate description of solvent–solute interactions than those based on simple spherical or ellipsoidal cavity [1, 3]. For molecular-shape cavities, several promising approaches have been introduced. In particular, the SMx models [1], which are based on the generalized Born formal-

* To whom correspondence should be addressed.

† On leave from the Institute of Chemical Physics, University of Latvia, 19 Rainis, Blvd., Riga, LV 1586, Latvia.

ism within the semiempirical molecular orbital theory, are quite successful in calculating free energy of solvation. However, the deficiency of the semiempirical molecular orbital wave function makes them less useful for modeling reactions in solution. Thus, to model reactions in solution, more accurate representation of the solute is required such as using DFT or ab initio molecular orbital theories. In this case, one can use the DFT/PB model [4–7], which combines DFT for solute density distribution and the Poisson–Boltzmann (PB) method for interaction with the dielectric continuum medium. Alternatively, the polarizable continuum model (PCM) [3, 8] can be employed. This model based on the Poisson boundary condition has been implemented at the DFT and ab initio MO levels of theory. Although both the DFT/PB and PCM models can provide accurate description of the solute in the dielectric cavity, their use is computationally rather expensive. Several approximations have also been developed. In the reaction field factors approach [9], the PCM equations are simplified by using multipole expansion for the solute density. We recently suggested the generalized conductor-like screening model (GCOSMO), which is based on the COSMO model originally proposed by Klamt and Schrümann within the semiempirical MO formalism [10]. In GCOSMO, accurate ab initio electronic wave function can be used for solute electrons and nonelectrostatic contributions are added to the free energy of solvation [11–14]. GCOSMO approximate boundary condition allows significant reduction in computational demand as compared to the DFT/PB and PCM-based models while maintaining comparable accuracy. Since DFT/PB, PCM, and GCOSMO models were implemented within the DFT and/or ab initio MO theory, they can be employed for quantitative modeling of reactions in solution. However, before extensive use of these models to real systems, thorough analyses of their accuracy should be performed.

Accuracy of continuum solvation models depends on (1) boundary conditions on the surface of the cavity, (2) the atomic radii used in determining the cavity size, and (3) the validity of the continuum approximation itself. In this study, we focus our attention on how these three factors affect the accuracy of the GCOSMO model.

The GCOSMO model uses the boundary condition from a cavity in a conductor and then scales

the surface charges for a dielectric medium. This is fundamentally different from the exact boundary condition used in the PCM model. In our previous study [11], we have shown a good agreement between GCOSMO and PCM hydration energies for a large set of molecules and ions when the same atomic radii were used. This shows that the GCOSMO approximation is quite accurate for solvents with high dielectric constants such as water. However, in principle, the GCOSMO scaling procedure may yield errors for solvents with low dielectric constants, though no systematic analysis has been done. To estimate the magnitude of these errors, here we compare results from GCOSMO and PCM calculations with experimental data for the tautomeric equilibria between 2-hydroxypyridine and 2-pyridone in several solvents having a wide range of dielectric constants.

In our previous work [11], we optimized a set of atomic radii for construction of molecular cavities for both GCOSMO and PCM calculations. With these atomic radii, GCOSMO model reproduces experimental hydration energies with an average unsigned difference of about 1 kcal/mol for neutral solutes and of order 2–4 kcal/mol for ions that were used in the fit. It is desirable to test applicability of these radii for a larger set of molecules and ions that were not included in the fit. In this study, we calculated hydration free energies for 39 molecules and 5 ions playing an important role in protein structure and function.

Finally, in this study, we perform a GCOSMO study on hydration effects on the potential surface for the proton transfer reaction in the $[\text{H}_3\text{N}-\text{H}-\text{NH}_3]^+$ system. Comparison of these results with previous QM/MM Monte Carlo simulations [15] provides a test of the applicability of the GCOSMO model for modeling of reaction profiles in solutions and also illustrates the use of GCOSMO gradient in determining geometries of stationary points on the free energy surface.

This study is organized as follows. In the theory section we present a brief overview of the GCOSMO model. The application section is divided into three parts: the first examines solvent effects on the tautomeric equilibria of 2-hydroxypyridine/2-pyridone in different solvents. The second provides a test of fitted atomic radii by calculating free energies of solvation for a large number of molecules and ions which were not studied by the GCOSMO earlier. The third discusses hydration effects on the potential surface the proton

transfer reaction in the $[\text{H}_3\text{N}-\text{H}-\text{NH}_3]^+$ system. Finally, conclusions and future directions are given.

Theory

GENERALIZED CONDUCTOR-LIKE SCREENING MODEL (GCOSMO)

The GCOSMO model is a generalization of the semiempirical COSMO method [10] to have an accurate ab initio description for the solute charge density and also to include dispersion, repulsion, and cavity formation contributions to the free energy. The GCOSMO model was incorporated into classical ab initio MO and DFT frameworks. The central approximation of this model is to scale the screening conductor surface charge by a factor of $f(\epsilon) = (\epsilon - 1)/\epsilon$ to satisfy the Gauss theorem for the total surface charge for a solute in a dielectric medium specified by the dielectric constant ϵ . The screening conductor surface charge can be obtained directly from the boundary condition that the total potential on the surface of the cavity in a conductor is zero:

$$\sum_i \frac{z_i}{|\mathbf{R} - \mathbf{R}_i|} - \int_V \frac{\rho(\mathbf{r}')}{|\mathbf{r} - \mathbf{r}'|} d^3r' + \int_S \frac{\sigma(\mathbf{r}')}{|\mathbf{r} - \mathbf{r}'|} d^2r' = 0, \quad (1)$$

where z_i and \mathbf{R}_i are values and positions of N nuclear charges, $\rho(\mathbf{r})$ is the solute electronic density and the solvent reaction field is represented by the surface charge density $\sigma(\mathbf{r})$.

Within the boundary element approach, a cavity boundary is defined by M surface elements with areas $\{S_u\}$. The surface charge density at each surface element is approximated as a point charge, $\{q_u\}$, located at the center of that element, $\{\mathbf{t}_u\}$. The surface charge distribution is then given by

$$\mathbf{q} = -f(\epsilon)\mathbf{A}^{-1}(\mathbf{B}\mathbf{z} + \mathbf{c}), \quad (2)$$

where \mathbf{A} , \mathbf{B} , and \mathbf{c} are $M \times M$, $M \times N$, and $M \times 1$ matrices, respectively, with matrix elements defined by [10]

$$A_{uv} = \frac{1}{|\mathbf{t}_u - \mathbf{t}_v|} \quad \text{for } u \neq v \quad \text{and} \\ A_{uu} = 1.07 \sqrt{\frac{4\pi}{S_u}}, \quad (3)$$

$$B_{ui} = \frac{1}{|\mathbf{t}_u - \mathbf{R}_i|}, \quad (4)$$

$$c_u = - \int \frac{\rho(\mathbf{r})}{|\mathbf{r} - \mathbf{t}_u|} d^3r, \quad (5)$$

and \mathbf{z} is the vector of N nuclear charges. The total free energy of the whole system (solute + surface charges) is then given by

$$E_{\text{tot}} = \sum_{\mu\nu} P_{\mu\nu} \left(H_{\mu\nu} + \frac{1}{2} G_{\mu\nu} \right) - \frac{1}{2} f(\epsilon) \mathbf{z}^\dagger \mathbf{B}^\dagger \mathbf{A}^{-1} \mathbf{B} \mathbf{z} + E_{\text{nn}} + \Delta G_{\text{nonels}}, \quad (9)$$

where E_{nn} is the solute nuclear–nuclear repulsion. The solvent contributions to the one- and two-electron terms of the Fock matrix elements ($H_{\mu\nu}$ and $G_{\mu\nu}$, respectively) are expressed as

$$H_{\mu\nu}^s = -f(\epsilon) \mathbf{z}^\dagger \mathbf{B}^\dagger \mathbf{A}^{-1} \mathbf{L}_{\mu\nu}, \quad (10)$$

$$G_{\mu\nu}^s = -f(\epsilon) \mathbf{c}^\dagger \mathbf{A}^{-1} \mathbf{L}_{\mu\nu}, \quad (11)$$

where

$$L_{\mu\nu}^u = - \left\langle \mu \left| \frac{1}{|\mathbf{r} - \mathbf{t}_u|} \right| \nu \right\rangle, \quad (8)$$

and $P_{\mu\nu}$ is the density matrix element; ΔG_{nonels} is the non-electrostatic part of the free energy of solvation that includes the dispersion, repulsion, and cavity formation contributions. For the dispersion and short-range repulsion contributions, we adopted Floris et al. method [16]. For the cavity formation term, we employed the scaled particle fluid theory of Pierotti [17], which was transformed by Huron and Claverie [18] into an atom-molecule-type formalism. Other non-electrostatic contributions—such as an entropy change due to the solvent reorganization, an enthalpy change due to changes in the solute vibrational and rotational degrees of freedom, a charge transfer to the solvent, non-electrostatic components of the solute–solvent hydrogen bonding, etc.—are effectively included in the atomic radii defining the cavity boundary. The cavity boundary was defined by the solvent-excluding surface (also known as molecular surface) proposed by Richard [19]. Note

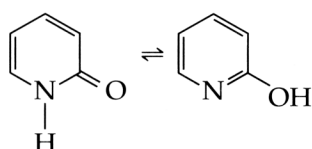
that in some cases when the solute can make strong hydrogen bonds with solvent molecules, the GCOSMO approach can be improved by including several explicit solvent molecules. This will be discussed more details in a separate report.

We have implemented the above formalism into the HF, MP2, CIS, and local and non-local DFT theories. Our results indicate that GCOSMO solvation energy gradient and Hessian calculations on the average require only about 10–20% more computational time as compared to corresponding gas-phase calculations. This is noticeably faster than other existing ab initio MO or DFT dielectric continuum models based on a general cavity.

Applications

TAUTOMERIC EQUILIBRIA OF 2-HYDROXYPYRIDINE/2-PYRIDONE IN SOLUTIONS

Tautomeric equilibria of heterocyclic compounds in solution are very sensitive to the solvent–solute interaction, thus providing excellent tests for accuracy of different solvation models. These properties have also been the subjects of recent reviews [1, 2, 20] due to their importance in biological systems. In this study, we consider the tautomeric equilibria of 2-hydroxypyridine/2-pyridone in different solvents as shown below:



Previous studies showed that almost all dielectric continuum models correctly predict the differential free energies of solvation for this system. We use this well-behaved system here mainly to test the accuracy of GCOSMO boundary condition and optimized atomic radii for solvents other than water by comparing our results with experimental data and with PCM calculations which employs an exact Poisson dielectric continuum boundary condition. We refer readers to an excellent review by Cramer and Truhlar for more discussion on the accuracy of other continuum solvation models for this system [2].

Gas-phase geometries for both 2-hydroxypyridine and 2-pyridone were optimized at the sec-

ond-order Møller–Plesset perturbation theory level using the 6-31G** basis set. These structures were used in solvation calculations for solvents with dielectric constants ϵ equal to 2, 5, 36, and 78, which correspond to cyclohexane, dimethyl ether, acetonitrile, and water, respectively. Free energies of solvation were calculated by using both PCM and GCOSMO models with our atomic radii. The van der Waals surface was used for the PCM model as implemented in the Gaussian 94 program. We found that the non-electrostatic terms contribute only about 0.1 kcal/mol in the calculated differential free energies of hydration, thus they were not included here.

Calculated differential free energies of solvation are listed in Table I along with experimental data [21]. For $\epsilon = 5$, the PCM surface charges do not converge for 2-hydroxypyridine. This convergent problem is due to the iterative procedure for calculating surface charges. Recent closure relation and matrix inversion formulations of the PCM model [22] may elevate this problem. For aqueous solvent, GCOSMO yields the error of 0.8 kcal/mol compared to the experiment. As expected, the GCOSMO surface charge scaling approximation produces larger errors for less polar solvents. It should be noted that both 2-hydroxypyridine and 2-pyridone have hydrogen bonding groups which would have strong interactions with first-solvation-shell waters. A good agreement with experimental data may result from cancelation of errors from specific hydrogen bond effects in both tautomers that were not included in the present and previous continuum calculations. A detailed analysis of modeling hydrogen bonding effects in conjunction with the dielectric continuum approach will be presented in a forthcoming study. The agreement between GCOSMO and PCM results for

TABLE I
Difference between free energies of solvation (kcal/mol) for 2-hydroxypyridine and 2-pyridone in solutes with different dielectric constant ϵ .

Model/Hamiltonian/Basis	$\epsilon = 2$	$\epsilon = 5$	$\epsilon = 36$	$\epsilon = 78$
GCOSMO/MP2/6-31G**	2.0	3.8	4.9	5.1
PCM/MP2/6-31G**	1.6	NC ^b	4.5	4.7
Experiment ^a	1.1	1.8	3.8	4.3

^a Ref. [21].

^b Not converged.

a wide range of solvents not only validates the boundary approximation used in GCOSMO but also opens the possibility for more quantitative quantum continuum solvation studies.

HYDRATION FREE ENERGIES

Using our recently optimized atomic radii (H: 1.172; C_{σ} : 2.096; $C_{\sigma\pi}$: 1.635; N_{hb} : 1.738; N_{nhb} : 2.126; O: 1.576; F: 1.28; P: 2.279; S: 2.023; Cl: 1.75) [11], we have calculated hydration free energies for a set of 39 neutral molecules and 5 ions which are of interest in biochemistry. GCOSMO calculations were done at the HF/6-31G* level using the gas-phase optimized geometries at the same level of theory. For dispersion and repulsion interactions between the solute with solvent water hydrogen and oxygen atoms, coefficients are taken from the OPLS force field [23]. Recall that in our previous study [11] we found rather small differences between hydration free energies calculated at the HF, DFT, and MP2 levels. Thus, we expect that DFT and MP2 theories would show the same trend as the present HF results. The calculated HF/6-31G* hydration free energies are listed in Table II along with available experimental data. We found that GCOSMO yields hydration free energies for neutral nonaromatic molecules with a RMS (root-mean square) difference with experiments of about 1.3 kcal/mol. This is consistent with our previous finding. An interesting new result is that for aromatic molecules, GCOSMO tends to overestimate the hydration free energies with a RMS error of about 2.6 kcal/mol. A careful examination of the fitting procedure [11] for atomic radii shows that the sp^2 carbon radius (1.635 Å) attempts to account for both hydrogen bonding effects in acids, acetones, and amides as well as resonance effects in aromatic compounds. However, the sp^2 carbon radius is biased toward the former since it has more experimental values used in the fit. Consequently, the sp^2 carbon radius is too small and effectively overestimates the resonance effects for aromatic compounds. For ions, the RMS error is about 5 kcal/mol, which is about the same range as in our previous study. Note that the wave functions for anions are quite diffuse. As a result, there is a non-negligible portion of the solute electron density outside of the cavity; this yields consistently smaller hydration free energies for anions as seen in Table II. Therefore, more accurate fitting of atomic radii is required with the use of carefully selected set of target species.

TABLE II
Calculated and experimental hydration free energies (in kilocalories per mole).

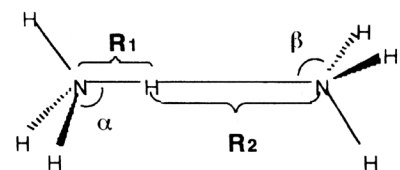
Solutes	$\Delta G_{\text{hyd}}^{\text{HF}}$	$\Delta G_{\text{hyd}}^{\text{exp}}$
<i>Neutral (nonaromatic)</i>		
Ethanol	-4.90	-4.9
1-Propanol	-4.39	-4.8
Isopropanol	-4.46	-4.8
Dimethylamine	-1.77	-4.3
Ethylthiol	-1.32	-1.3
Methyl-ethylsulfide	-1.88	-1.5
Dimethylsulfide	-0.94	-1.4
Diethylsulfide	0.25	-1.3
Butanone	-3.89	-3.6
2-Pentanone	-3.70	-3.5
3-Pentanone	-2.82	-3.4
Acetaldehyde	-4.58	-3.5
Propionic acid	-7.78	-6.5
acetamide	-11.36	-9.7
Propionamide	-10.35	-9.4
N-methylacetamide	-8.97	-10.0
N-p-Guanidine	-11.61	-11.0
Trimethylamine	0.19	-3.2
1-Propylamine	-2.89	-4.4
2-Methoxyethanol	-6.70	-6.8
2-Methoxypropane	-0.19	-2.0
3-pentanone	-3.64	-3.4
Ethylacetate	-4.27	-3.1
Methyl-butanoate	-3.39	-2.8
Methyl-propanoate	-4.02	-2.9
Methylformate	-5.40	-2.8
N-methylacetamide	-9.04	-10.0
Piperazine	-5.77	-7.4
Pro-2-en-1-ol	-4.64	-5.0
RMS error	1.27	
<i>Neutral (aromatic)</i>		
Benzene	-2.95	-0.9
Toluene	-2.01	-0.9
4-Methylpyridine	-2.76	-4.9
P-cresole	-7.91	-6.1
2-Methylphenol	-7.72	-5.9
Methylindole	-7.47	-5.9
Methylimidazole	-11.42	-10.0
Aniline	-7.28	-4.9
Acetophenone	-8.47	-4.6
Benzaldehyde	-9.29	-4.0
RMS error	2.64	
<i>Ions</i>		
N-Butylammonium	-63.6	-69
Methyl-thiol ion	-72.4	-74
Propionate ion	-73.4	-79
P-cresole ion	-66.5	-75
Methylimidazolium	-66.9	-64
RMS error	5.4	

SOLVENT EFFECTS ON POTENTIAL ENERGY SURFACE FOR THE PROTON TRANSFER IN $\text{H}_3\text{N}\dots\text{HNH}_3^+$

Proton transfer reactions are fundamentally important in many chemical and biological processes and are the subjects of numerous theoretical and experimental studies. Since proton transfer in biological systems occurs under the influence of the protein and aqueous environments, environmental effects are of profound importance for modeling its reaction mechanisms. In this study, we provide an analysis of the potential energy surface of the proton transfer in the $\text{H}_3\text{N}\dots\text{HNH}_3^+$ system in aqueous solution, which is often being used as a model for proton transfer in biological systems. In particular, McCammon and co-workers [24] have constructed an analytical potential function for the gas-phase reaction based on the MP2/6-31G* energies and pointed out that the N–N vibration of the donor and acceptor fragments has a noticeable effect on the barrier to proton transfer. Gao [15] has performed hybrid QM/MM simulations based on the AM1 semiempirical Hamiltonian for the quantum region to obtain a two-dimensional potential energy surface for this reaction and noted that hydration effects further raise the barrier at large N–N distances.

Geometries of the ion–dipole complex and saddle point were fully optimized at the MP2/6-31G** level of theory in both the gas phase and in aqueous solution. Optimized geometrical parameters and barrier heights are listed in Table III. We found that the aqueous environment has a significant effect on the geometry of the ion–dipole complex due to the large total dipole but has a little effect on the structure of the zero-dipole transition state, even though the difference in hydration energies of the complex and transition state is only 1.5 kcal/mol. In particular, the NH_i bond distance (R_1) of the ammonium shortens from 1.134 to 1.058 Å while the hydrogen bond (R_2) elongates from 1.533 to 1.801 Å when transferring from the gas phase to aqueous solution. This is consistent with previous finding on the similar $[\text{H}_2\text{O}\dots\text{H}\dots\text{OH}_2]^+$ system using the PCM solvation model [25]. As pointed out in previous studies [15, 25], the charge distribution is more delocalized at the transition state; consequently the transition state is less solvated compared to that of the ion–dipole complex. This leads to an increase in the proton transfer barrier by 1.5 kcal/mol from its values in the gas phase of 0.45 kcal/mol. Similar

TABLE III
 Geometrical parameters (bond lengths in angstroms and angles in degrees) of stationary points and barrier heights (kilocalories per mole) to proton transfer in both the gas phase and aqueous solution.



	Gas phase		Solution	
	Complex	TS	Complex	TS
R_1	1.134	1.298	1.058	1.296
R_2	1.533		1.801	
α	110.7	111.8	109.9	111.7
β	112.7		112.8	
ΔE or $\Delta\Delta G$	0.0	0.45	0.0	1.94
ΔG_{solv}			70.4	68.9

increase of 1.24 kcal/mol was found for the barrier of the proton transfer in the $[\text{H}_2\text{O}\dots\text{H}\dots\text{OH}_2]^+$ system using the PCM solvation model [25]. However, our result is a factor of 2 smaller than Gao's prediction of 3 kcal/mol using QM/MM–AM1/OPLS approach [15]. This difference could result from several factors. One is the solvent–solute hydrogen bond effects which is treated in an average manner in our continuum calculations. But including specific first-solvation-shell hydrogen bond effects in a discrete continuum model was found to lower the proton transfer barrier for the $[\text{H}_2\text{O}\dots\text{H}\dots\text{OH}_2]^+$ system [25]. The other factor is the difference in the solute electronic wave functions, MP2 in our calculations as compared to AM1 in Gao's simulations [15]. However, as mentioned earlier, our previous study [12] showed that solvation energy is not very sensitive to the quality of the solute wave function (though only HF, MP2, and DFT levels were considered). More study is certainly needed to sort out the origins of this discrepancy.

To provide a quantitative understanding of the hydration effects on the potential energy surface of this reaction particularly along the N–N stretching mode, we have calculated the potential curves for proton transfer between two nitrogen atoms separated by distances $R_{\text{NN}} = 2.5, 2.75,$ and 3 Å, respectively, both in the gas phase and in aqueous

solution. Since the spectator R_{NH} bond distances and HNN angles remain nearly constant about 1.02 Å and 111.6°, respectively, at the reactant and transition state, they are assumed to be fixed. These potential curves plotted versus the reaction coordinate are shown in Figure 1. The reaction coordinate used here is defined as the difference in the distances from the transferring proton to the acceptor and the donor nitrogens. In general, our results agree well with those obtained from QM/MM Monte Carlo simulations by Gao. In particular, at $R_{NN} = 2.5$ Å, the free energy surface is barrierless to proton transfer. However, as the N–N distance increases the barrier to proton transfer also increases but at a faster rate in the presence of aqueous solvent. Furthermore, the ion–dipole complex is more stabilized by the aqueous solvent as the N–N distance increases making the complex minimum flatten out relative to that of the gas-phase minimum. These features have been discussed in details by Gao. The general agreement between our results and those from Gao's QM/MM simulations [15] leads to an important conclusion that the simple and efficient GCOSMO model can be used effectively for reaction profile calculations instead of expensive simulations. This allows one to use more sophisticated quantum mechanical methods that is essential for quantita-

tive description of bond-breaking and -forming processes in solution and to consider realistic reacting systems with reasonable computational cost. In addition, the availability of GCOSMO first and second energy derivatives allows one to study solvent effects on the reaction coordinates which have not been addressed in the past. Such effects will be discussed in a forthcoming study.

Conclusion

The GCOSMO continuum solvation model has shown considerable promise in modeling equilibria, structure, and reactivity of reactions in solutions. In many cases, like tautomeric equilibrium in 2-hydroxypyridine/2-pyridone and proton transfer reaction in the $H_3N-H-HN_3^+$ system studied here, the use of the dielectric continuum GCOSMO model is justified, as shown by comparison with more rigorous PCM and QM/MM results. In such cases, the main advantage of the GCOSMO model is the computational efficiency in calculating solvation free energy and its derivatives. The accuracy of about 1 kcal/mol for hydration free energies of neutral nonaromatic solutes and slightly larger for aromatic solutes and ions is comparable to the more rigorous PCM model. More work is needed to improve the atomic radii for defining the cavity and to include specific hydrogen bonding effects. Extending this model to study solvent effects on electronic absorption and vibrational spectra is currently under way in our laboratory.

ACKNOWLEDGMENT

This work is supported in part by the University of Utah and by the National Science Foundation through a Young Investigator Award to T.N.T.

References

1. C. J. Cramer and D. G. Truhlar, in *Reviews in Computational Chemistry*, K. B. Lipkowitz and D. B. Boyd, Eds. (VCH Publishers, New York, 1994) p. 1.
2. C. J. Cramer and D. G. Truhlar, in *Solvent Effects and Chemical Reactivity*, O. Tapia and J. Bertrán, Eds. (Kluwer, Dordrecht, 1996) p. 1.
3. J. Tomasi and M. Persico, *Chem. Rev.* **94**, 2027 (1994).
4. J. L. Chen, L. Noodleman, D. A. Case, and D. Bashford, *J. Phys. Chem.* **98**, 11059 (1994).

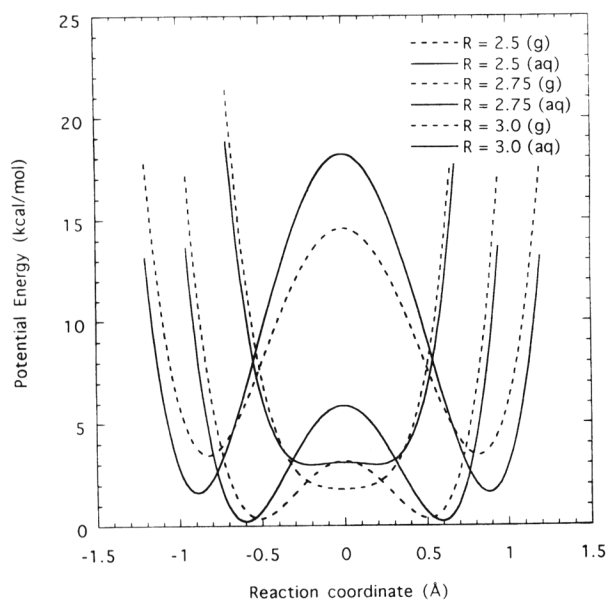


FIGURE 1.

TRUONG, NGUYEN, AND STEFANOVICH

5. A. A. Rashin, M. A. Bukatin, J. Andzelm, and A. T. Hagler, *Biophys. Chem.* **51**, 375 (1994).
6. D. J. Tannor, B. Marten, R. Murphy, R. A. Friesner, D. Sitkoff, A. Nicholls, M. Ringnalda, W. A. Goddard, and B. Honig, *J. Am. Chem. Soc.* **116**, 11875 (1994).
7. K. Baldrige, R. Fine, and A. Hagler, *J. Comp. Chem.* **15**, 1217 (1994).
8. S. Miertus, E. Scrocco, and J. Tomasi, *Chem. Phys.* **55**, 117 (1981).
9. V. Dillet, D. Rinaldi, and J. L. Rivail, *J. Phys. Chem.* **98**, 5034 (1994).
10. A. Klamt and G. Schüürmann, *J. Chem. Soc., Perkin Trans. II*, 799 (1993).
11. E. V. Stefanovich and T. N. Truong, *Chem. Phys. Lett.* **244**, 65 (1995).
12. T. N. Truong and E. V. Stefanovich, *Chem. Phys. Lett.* **240**, 253 (1995).
13. T. N. Truong and E. V. Stefanovich, *J. Phys. Chem.* **99**, 14700 (1995).
14. T. N. Truong and E. V. Stefanovich, *J. Chem. Phys.* **103**, 3709 (1995).
15. J. Gao, In *Reviews in Computational Chemistry*, K. B. Lipkowitz and D. B. Boyd, Eds. (VCH Publishers, New York, 1996) p. 119.
16. F. M. Floris, J. Tomasi, and J. L. P. Ahuir, *J. Comp. Chem.* **12**, 784 (1991).
17. R. A. Pierotti, *Chem. Rev.* **76**, 717 (1976).
18. M. J. Huron and P. Claverie, *J. Phys. Chem.* **76**, 2123 (1972).
19. F. M. Richards, *An. Rev. Biophys. Bioeng.* **6**, 151 (1977).
20. J. S. Kwiatkowski, T. J. Zielinski, and R. Rein, *Adv. Quantum Chem.* **18**, 85 (1986).
21. P. Beak, *Acc. Chem. Res.* **10**, 186 (1977).
22. E. L. Coitiño, J. Tomasi, and R. Cammi, *J. Comp. Chem.* **16**, 20 (1995).
23. W. L. Jorgensen and J. Tirado-Rives, *J. Am. Chem. Soc.* **110**, 1657 (1988).
24. L. Jaroszewski, B. Lesyng, J. J. Tanner, and J. A. McCammon, *Chem. Phys. Lett.* **175**, 282 (1990).
25. F. R. Tortonda, J. L. Pascual-Ahuir, E. Silla, and I. Tuñon, *J. Phys. Chem.* **97**, 11087 (1993).